



1 **Effect assessment of NO_x and SO₂ control policies on acid species in precipitation from 2005 to**
2 **2016 in China based on satellite monitoring**

3 Xiuying Zhang ^{1,*}, Dongmei Chen ^{2,3}, Lei Liu ^{1,4}, Limin Zhao ¹, Wuting Zhang ¹

4 ¹ International Institute for Earth System Science, Nanjing University, Nanjing 210023, China

5 ² Department of Geography and Planning, Queen's University, Kingston, ONK7L 3N6, Canada

6 ³ School of Geography and Remote Sensing, Nanjing University of Information Science & Technology,
7 Nanjing, China

8 ⁴ Jiangsu Center for Collaborative Innovation in Geographical Information Resource Development and
9 Application, Nanjing 210023, China

10 * Corresponding authors: Xiuying Zhang (lzhxy77@163.com)

11 **Abstract**

12 The effects of NO_x and SO₂ policies on acid species in precipitation was assessed in China from 2005
13 to 2016, based on the OMI measured SO₂ and NO₂ columns. The results showed that the SO₂ and NO₂
14 columns in the atmospheric boundary layer (ABL) could be used to indicate the variations of S / N in
15 precipitations (R = 0.90, incept = 0.97, P < 0.05). The spatial distribution of S / N was lower in eastern
16 China than the west, which had a negative logarithmic relationship with population densities (R = 0.78,
17 P < 0.05). The OMI-derived S / N decreased significantly from 2005 to 2016 (17.21 and 10.70 in 2005
18 and 2016, respectively), mainly due to the controlling S and N policies enacted at different times. The
19 ABL SO₂ columns showed a decreasing trend from 2005 to 2016, while NO₂ presented an increasing
20 tendency from 2005 to 2011 then decreasing until 2016. The temporal variations of SO₂ and NO₂ were
21 not only determined by their emissions but also affected by precipitation amount, which induced the
22 highest SO₂ and NO₂ concentrations in 2011 during the study time. With the combined acidification



23 effects of S and N, the acidity had increased from 2005 to 2011, then decreased until 2016. The acidity
24 in 2016 has declined 11.0% and 25.4%, respectively, compared with those in 2005 and 2011, indicating
25 the policies on joint controlling SO₂ and NO₂ have gained effects.

26 **Keywords:** Acid species, precipitation, policies, China, remote sensing, OMI

27 1. Introduction

28 The economic growth in recent 30 years in China has been accompanied by increased energy demand
29 and massive emissions of pollutants (Kuribayashi et al., 2012). Among them, sulfur dioxide (SO₂) and
30 nitrogen dioxide (NO₂) are important precursors of acid rain. After released into the atmosphere, SO₂
31 and NO₂ can be transformed into nitrate (NO₃⁻) and sulfate (SO₄²⁻) through complex physical and
32 chemical processes (Yu et al., 2016), and then diluted with precipitation. Increased acid deposition and
33 the followed decreased pH of precipitation, directly and indirectly, influence the eco-environments
34 (Charlson and Rodhe, 1982; Li et al., 2017; Larssen and Carmichael, 2000). Currently, China is
35 becoming one of the highest acid deposition areas on a global scale (Vet et al., 2014), which has been
36 drawing serious concerns from the public and policy makers in China due to the adverse impacts of
37 acid rain on the ecological environment.

38 To control acid rain pollution, the Chinese government has implemented a series of policies from the
39 9th to 12th Five-Year Plans (1996-2015). “Decision of the State Council on Several Issues Concerning
40 Environmental Protection” was issued in 1996, in which “15 major categories of small pollutant
41 enterprises” related to pollutant emissions should be closed ([1996]31). In 1998, the Chinese
42 government adopted national legislation, known as the “two control zones (TCZs) plan”, to limit
43 ambient SO₂ pollution and halt the increase of acid rain. During the 11th Five-year Plan, a clear aim was
44 announced that national wide SO₂ emission in 2010 should be reduced by 10% of that in 2005, and the



45 increasing tendency of NO_x should be controlled. Under such strict policies, small power generating
46 units and inefficient industrial facilities were closed, and 82.6% of the thermal power plants were
47 equipped with flue gas desulfurization (FGD) in 2010 (China Environmental Bulletin 2010). However,
48 the ground measurements of precipitation pH indicated that the control policies had not been successful
49 in reducing acid rains (China Environmental Bulletin 2010). Thus several studies have argued whether
50 it is enough to control acid rain pollutions through only controlling SO_2 emissions (Zhao et al.,
51 2009;Fang et al., 2013).

52 To further improve the air quality and control acid rains, the Chinese government issued “Twelfth
53 Five-Year Plan for National Environment Protection” in 2011, and set a goal to reduce the emissions of
54 NO_x by 10% and SO_2 by 8% in 2015. Additionally, the Ministry of Environmental Protection, National
55 Development and Reform Commission, and Ministry of Finance jointly issued “12th Five-Year Plan on
56 air pollution prevention and control in Key regions” in 2012, which aims to reduce the emissions of
57 SO_2 and NO_x by 12% and 13%, and the concentrations of SO_2 and NO_2 by 10% and 7% in the key
58 regions in 2015. Selective catalytic reduction (SCR) equipment was recommended to install in this
59 period and the SCR equipment number grew from a percentage of about 18% in 2011 to 86% in 2015
60 (Liu et al., 2016a). Moreover, several new national emission standards for cars have been implemented
61 to reduce the NO_x emissions generated by traffics (Wu et al., 2017).

62 Several studies have discussed the effect of environmental protection policies on the emissions,
63 concentrations, and depositions of S and N in China, based on the ground measurements or satellite
64 monitoring information (Kuribayashi et al., 2012;Krotkov et al., 2016;Zhao et al., 2013;Ronald et al.,
65 2017;de Foy et al., 2016). It was found that SO_2 emissions in China increased continuously before 2006,
66 and declined after 2006 due to wide application of flue-gas desulfurization (FGD) in power units since



67 2005 (Fang et al., 2013;Duan et al., 2016). NO_x emission was also found to have a rapid increase from
68 1990 to 2011 and decreased from 2012 because of the broad applications of SCR in coal-fired power
69 plants (Wang et al., 2014). The remotely sensed SO₂ and NO₂ columns also showed that FGD had a
70 significant effect when a much stricter control of the actual use of the installations began in the years of
71 2008-2009 (Ronald et al., 2017). The remotely sensed NO₂ columns reached the peak in 2011 and then
72 decreased from 2012 in China (Chen et al., 2017). But the emission peak years for NO₂ varied from
73 province to province (Ronald et al., 2017). Although the peak years for SO₂ and NO₂ varied in different
74 studies, these studies confirmed that atmospheric S and N increased first due to the economic
75 development, and then decreased because of the enacted policies.

76 The different changing steps of S and N in the atmosphere, including the different increasing /
77 decreasing rates and peak years, directly influence the S and N depositions through precipitation
78 (Huang et al., 2009;Liu et al., 2016d;Liu et al., 2016c). According to a review on chemical
79 compositions precipitation in recent years, the pollution in precipitation is still dominated by sulfur
80 type with a trend to sulfuric-nitrous mixed type in China (Wang and Xu, 2009). The declined ratio of
81 SO₄²⁻ to NO₃⁻ concentration has been observed in northern China (Wang et al., 2012;Pu et al., 2017),
82 southeast China (Huang et al., 2008;Fang et al., 2013), and southwest China (Liu et al., 2016b),
83 indicating the proportion of NO₃⁻ concentration on precipitation acidity has been increased in
84 recent years. Combining the acidification effects of S and N, the benefits of SO₂ reductions during
85 2005–2010 might be largely offset by increases of N emissions (Zhao et al., 2009) However, the
86 change of the contributions of SO₄²⁻ and NO₃⁻ on precipitation acidity has not been evaluated,
87 particularly on a national scale.

88 Compared with the ground measurements, the remote sensing technique provides a new means to



89 monitor the concentrations of SO₂ and NO₂ in the atmosphere, with the advantages of extensive spatial
90 details and continuous temporal coverage (Zyrichidou et al., 2013). At present, the Global Ozone
91 Monitoring Experiment (GOME2A, 2007-; GOME2B, 2013-), Scanning Imaging Absorption
92 Spectrometer for Atmospheric Cartography (SCIAMACHY, 2002-2012), and the Ozone Monitoring
93 Instrument (OMI, 2004-) on the Aura satellite provide both of the SO₂ and NO₂ column products.
94 Among them OMI provides the smallest instantaneous ground pixel resolution (13×24 km² at nadir)
95 and its products have been widely used for studying the spatial and temporal variations of SO₂ and NO₂
96 concentrations in the atmosphere and evaluating the effects of policies (Ronald et al., 2017; Chen et al.,
97 2017; Krotkov et al., 2016; Song and Yang, 2014; de Foy et al., 2016; Lamsal et al., 2015). However, few
98 studies have used the remotely sensed SO₂ and NO₂ columns data to indicate the variations of acid
99 components in precipitation (Liu et al., 2017; Zhang et al., 2012).

100 Remotely sensed SO₂ and NO₂ columns have been used to study the effect of precipitation variation on
101 severe acid rains in southern China (Xie et al., 2009), and evaluate the influence of SO₂ and NO₂
102 columns on precipitation pH in Anhui and Liaoning Provinces (Shi et al., 2010; Zhang et al., 2012).
103 More particularly, Liu et al. estimated monthly NO₃⁻¹ deposition through precipitation using the OMI
104 NO₂ columns and precipitation amount (Liu et al., 2017). In their work, the atmospheric boundary layer
105 (ABL) NO₂ columns below the precipitation height instead of the tropospheric NO₂ columns were used
106 to construct the statistical model to estimate NO₃⁻¹ depositions, since the scavenging effect on N
107 compounds is from the top precipitation height rather than the top troposphere height (Racette et al.,
108 1996). Therefore, the ABL SO₂ and NO₂ columns should be better than tropospheric columns when
109 indicating the acid components deposited.

110 Based on the ABL SO₂ and NO₂ columns, this study aims to evaluate the trends of the contributions of



111 the sulfate and nitrate ions on the acidity of precipitation from 2005 to 2016, under the policies enacted
112 and economic development in China. First, the remotely sensed indicator of S / N to the ratio of sulfate
113 and nitrate ions in rainwater is constructed based on ABL SO₂ and NO₂ columns; second, the spatial
114 variations and the trends of the S / N in rainwater are detected; finally, the spatial and temporal
115 variations of the potential acidification by sulfate and nitrate ions are evaluated.

116 2. Materials and methods

117 2.1. Materials used in this study

118 2.1.1. Tropospheric NO₂ and ABL SO₂ columns from OMI

119 The OMI satellite instrument is a nadir-looking UV-visible spectrometer on the Aura satellite (Levelt et
120 al., 2006). Aura was launched on 15 July 2004 and flies in a sun-synchronous polar orbit with a local
121 equatorial overpass time of 13:40 on the ascending node. The NO₂ columns are provided in the publicly
122 released level 2.0 (DOMINO 2.0) (<http://www.temis.nl>), which has greatly improved the accuracy of
123 the tropical NO₂ columns of the version 1.0 (Boersma et al., 2011). A new data set of ABL SO₂
124 columns from OMI is available, which agree on average within 12% with ground observations,
125 strongly improved on earlier SO₂ data sets from satellites (Theys et al., 2015).

126 In this study, the monthly tropospheric NO₂ columns from Jan 2005 to Dec 2016 over China are used.

127 The missing data is interpolated using IDW (Inverse Distance Weight) method, and then the unit of DU
128 (Dobson unit) for SO₂ column is transformed to molec. cm⁻² by multiplying 2.6875×10^{16} molec. cm⁻²
129 ($1\text{DU} = 2.6875 \times 10^{16}$ molec. cm⁻²) (Lee et al., 2011). Finally, the monthly mean SO₂ columns are
130 averaged from the daily data.

131 2.1.2. NO₂ profiles simulated from MOZART-4

132 The 56 levels of NO₂ concentrations in the atmosphere along altitudes from 2005 to 2016 have been



133 simulated from MOZART-4, a global chemical transport model. This model is driven by NCEP/NCAR
134 reanalysis meteorology and uses emissions based on POET (Precursors of Ozone and their Effects in
135 the Troposphere), REAS (Regional Emission inventory for Asia) and GFED2 (Global Fire Emissions
136 Database, version 2). Evaluation with several sets of observations shows that MOZART-4 can
137 reproduce tropospheric chemical composition with an acceptable accuracy (Emmons et al., 2010). The
138 output data used in the current work are temporally varying six hours every day, which are upon
139 request by Louisa Emmons at National Center for Atmospheric Research (NCAR)
140 (<http://www.acom.ucar.edu/wrf-chem/mozart.shtml>).

141 **2.1.3. Concentrations of SO_4^{2-} and NO_3^- in precipitation during 2005 - 2016 collected from the** 142 **published papers**

143 To test whether OMI-derived S/N could be used to indicate SO_4^{2-} / NO_3^- in precipitation, the SO_4^{2-} and
144 NO_3^- concentrations in precipitation during 2005-2016 in China from the published studies were
145 collected. The detailed information on searching the relevant papers has been detailed described in
146 those studies (Liu et al., 2016c; Liu et al., 2016d). Since the mentioned two studies collected the data
147 from 2000-2013, we removed the data from 2000 to 2004 and added the SO_4^{2-} and NO_3^- data published
148 during 2014-2016 in this study. In total, 168 records on annual SO_4^{2-} and NO_3^- concentrations in
149 precipitation have been selected.

150 **2.1.4 Spatial distribution of population density**

151 The spatial distribution of population density in 2010 in China is used to study the relationship between
152 the S / N and population density. The spatial resolution is $1 \text{ km} \times 1 \text{ km}$. This data set was produced by
153 integrating the physical geography factors and the statistical data on population in 2010, which is freely
154 downloaded from <http://www.geodoi.ac.cn/doi.aspx?doi=10.3974/geodb.2014.01.06.v1>.

155 **2.2. Methods**156 **2.2.1. Calculation of ABL NO₂ columns**

157 The MOZART-4 output of NO₂ concentrations includes 56 vertical levels from the ground to the top of
158 the troposphere. To simulate the profile of NO₂, a Gauss function is used:

$$159 \quad f(C_h^M) = \sum_{r=2}^n a^r \exp\left(\frac{-(h-b_r)^2}{c^2}\right) \quad (1)$$

160 where C_h^M is the NO₂ concentrations at the atmospheric height h ; a refers to the amplitude, b is the
161 centroid (location), c refers to the peak width, n is the number of peaks to fit. In this study, the models
162 with n from 2 to 6 are simulated, among which the model with the lowest RMSE (Root Mean Square
163 Error) and the highest R^2 is selected.

164 The tropospheric and ABL NO₂ columns ($\Omega_{trop}^M, \Omega_{ABL}^M$) simulated from MOZART-4 are simulated by
165 an integration method:

$$166 \quad \Omega_{trop}^M = \int_0^{trop} f(C_h^M) \quad (2)$$

$$167 \quad \Omega_{ABL}^M = \int_0^{ABL} f(C_h^M) \quad (3)$$

168 Then the OMI-derived ABL NO₂ column (Ω_{ABL}^O) is calculated as:

$$169 \quad \Omega_{ABL}^O = \Omega_{trop}^O \times \frac{\Omega_{ABL}^M}{\Omega_{trop}^M} \quad (4)$$

170 Where Ω_{trop}^O is the NO₂ columns retrieved from OMI.

171 **2.2.2. Calculation of the OMI-derived S / N to indicate the SO₄²⁻ / NO₃⁻ in precipitation**

172 In the study of Liu et al. (2017b), the NO₃⁻ deposition in precipitation ($D_{NO_3^-}$) could be estimated by the
173 following equation:

$$174 \quad D_{NO_3^-} = \alpha + \beta(\Omega_{ABL,N}^O \times P - \varepsilon) \quad (5)$$

175 Where α and β are the intercept and the slope of the constructed model, ε is the site bias, P is the
176 precipitation amount, and $\Omega_{ABL,N}^O$ is an indicator of N compounds in the atmosphere. Here, $\Omega_{ABL,N}^O$



177 refers to the ABL NO₂ columns.

178 Similarly, the SO₄²⁻ deposition in precipitation could be estimated by the similar equation format as Eq.

179 (5)¹. Here, we directly use the coefficients of β for N and S in the two studies to indicate the dilution

180 rates on N and S by precipitation, in which β for N and S was 9.33 and 7.10, respectively (Liu et al.,

181 2017).

182 Thus the OMI-derived S / N is calculated by :

$$183 \quad S / N = \frac{\beta_S \times \Omega_{ABL,S}^O}{\beta_N \times \Omega_{ABL,N}^O} \quad (6)$$

184 The correlation coefficient between the OMI-derived S / N and the collected data of SO₄²⁻ / NO₃⁻ in

185 precipitation is calculated to determine the degree to which the two data sets are associated. Other

186 parameters of relative error (RE) and absolute error (AE) are used to assess the accuracy of the

187 estimated NO₂ by the following function:

188 2.2.3. Potential acidity induced by H₂SO₄ and HNO₃

189 Generally, the precipitation acidity is due to H₂SO₄ and HNO₃, whereas HCl, HF, and other organic

190 acids are considered as negligible acidity contributors compared to H₂SO₄ and HNO₃ (He et al.,

191 2010; Khwaja and Husain, 1990). If all of the non-seasalt sulfate and NO₃⁻ presented in free acid forms,

192 the potential acidity could be estimated using the sum of nss-SO₄²⁻ and NO₃⁻ in precipitation (Rodhe et

193 al., 2002). Since the method and the simulated result on D_{NO₃⁻} have been well evaluated by Liu (Liu et

194 al., 2017), here we directly use the format of the equation to estimate the concentration in H⁺.

195 Since H₂SO₄ has two H⁺ while HNO₃ has one, the latent acidification effects could be calculated as

196 follows:

$$197 \quad PA = \beta_N \times \Omega_{ABL,N}^O + 2\beta_S \times \Omega_{ABL,S}^O \quad (7)$$

¹ This study has not been published yet.



198 Here PA is not an actual value of the concentration of H^+ induced by H_2SO_4 and HNO_3 , since equation
199 (7) does not calculate the S and N deposition through H_2SO_4 and HNO_3 . The PA is used here to indicate
200 the variation of H^+ induced by H_2SO_4 and HNO_3 for a long-term study.

201 3. Results and discussions

202 3.1. Validation of the OMI-derived S / N on SO_4^{2-} / NO_3^- in precipitation

203 The scatter plots of the OMI-derived S / N and SO_4^{2-} / NO_3^- is illustrated in Fig. 1(a). The OMI-derived
204 S / N has achieved a reasonably high predictive power on the ratio of SO_4^{2-} to NO_3^- in precipitation,
205 with a slope of 0.97 and R of 0.90. From Fig. 1(a), four points apparently deviated from the main trend
206 were located in Xizang, Yunnan, Guizhou, and Hainan provinces (Red circle in Fig 1(b)). If these
207 points were removed, the R would be increased from 0.90 to 0.94. This confirmed that the OMI derived
208 S / N could be used to indicate the variations of SO_4^{2-} / NO_3^- in precipitation across China.

209 The spatial distribution of the relative errors between the collected SO_4^{2-} / NO_3^- and OMI-derived S / N
210 components is shown in Fig.1 (b). The relative errors ranged from -56.2% to 210.4%, indicating the
211 ability of OMI-derived indicator on SO_4^{2-} / NO_3^- varied greatly across China. The average of the *RE*
212 and *AE* was -11.8 % and 22.0 % for the 168 data records, which denoted that the OMI-derived S / N
213 had underestimated the ratio of SO_4^{2-} / NO_3^- in precipitation. About 134 data records had the *RE* within
214 -30% to 30%, indicating 80% of the OMI-derived S / N at the collected sample locations could be used
215 to indicate the SO_4^{2-} / NO_3^- in precipitation. Eighteen and three data records had the *RE* between -45% -
216 -30% and 30% -45%, respectively. While six data records had very high *RE* values, particularly for the
217 sites in Southwestern China, which might be caused by the errors of the NO_2 and SO_2 columns derived
218 from OMI in these areas.



219 3.2. Spatial distribution of OMI-derived S / N in China

220 The spatial distribution of OMI-derived S / N in 2016 is illustrated in Fig. 2. The ratio ranged from 0.49
221 to 71.73, with an average of 10.70, which was much higher than the average of $\text{SO}_4^{2-} / \text{NO}_3^-$ in
222 precipitation (2.59) from 474 stations by ground measurements (China Environmental Bulletin 2016).
223 The big gap was mainly due to that 10.70 was the average of S / N for the whole China, while 2.59 was
224 calculated from the 474 measuring sites, most of which were located in urban areas. The average of
225 OMI-derived S / N at the 474 points was 2.78, which was very close to that $\text{SO}_4^{2-} / \text{NO}_3^-$ in
226 precipitation in 2016.

227 According to the classification standard on acid rain types (Cheng and Huang, 1998), 17.3% of the total
228 areas of China in 2016 had the acid rains of sulfuric-nitrous mixed types ($0.50 < \text{S} / \text{N} < 3$). The rest
229 82.7% had sulfuric acid rains ($\text{S} / \text{N} > 3$), among which 49.1% were contributed by the areas with S / N
230 values higher than 10. Since only several pixels had the S / N values lower than 0.50 (the minimum of
231 0.49 very close to 0.50), which have been neglected in this study. Thus, the precipitation acidity in
232 China is still mainly from the contribution of sulfuric species at present.

233 The large range of S / N indicated that a high variation of sulfate to nitrate components in precipitation
234 existed across China. The S / N values lower than 3 covered large areas from the northeast China to the
235 south China, including the whole province of Shandong, Jiangsu, Anhui, and Henan, and partly
236 provinces of Liaoning, Hebei, Shanxi, Shaanxi, Hubei, Hunan and Zhejiang. Also, in some local areas
237 around Urumqi, Lanzhou, Yinchuan in northeast China, Chengdu and Chongqing in Central China,
238 Nanning, Guangzhou and Taiwan in South China, Changchun and Harbin in Northeast China, the S / N
239 also presented low. Particularly, some areas around Beijing-Tianjin-Hebei, Shandong,
240 Shanghai-Jiangsu-Zhejiang, Guangdong, Hubei, Shaanxi, and Chongqing-Sichuan, had the S / N less



241 than 1, indicating the dominant acid component has changed from sulfate to nitrate. While in the
242 Qinghai-Xizang areas, the northern part of Inner Mongolia, and the south of Yunnan Province, the ratio
243 showed relative high.

244 The ratio of S / N was mainly determined by the different sources of SO₂ and NO_x. In fact, SO₂ and
245 NO_x are released by more or less the same anthropogenic sources, i. e. the burning of coal or oil,
246 volcanic activity, burning biomass. The main difference to SO₂ is that traffic is a much more important
247 source for NO_x (Ronald et al., 2017). The highly developed traffics in the densely populated areas, and
248 the more widespread application of the FGD than SCR in power units might be the main reasons for the
249 low values of S / N in the mentioned regions (Duan et al., 2016; Wang et al., 2014; Fang et al., 2013).

250 The spatial pattern of S / N is highly negatively correlated to that of population densities (Fig. 2b). To
251 illustrate the relationship between the population density and the ratio of S to N, the zonal means of S /
252 N were calculated by the different grades of population density (< 100, 100-200, 200-300, 300-400,
253 400-500, 500-1000, 1000-5000, 5000-10000 people/km²). It was found that the population density had
254 a significantly negative logarithmic relationship on S / N (Fig. 3). With the population density increases,
255 the S / N decreased. The population might not directly influence on the S / N, while it indirectly effects
256 on the emission source of S and N through human activities.

257 3.3. Long-term trends of the S / N from 2005 to 2016

258 The averages of the OMI-derived S / N, SO₂, NO₂ columns are shown in Fig. 4. In China, SO₂
259 concentrations in the atmosphere increased first from 2005 to 2007 and then declined with a little
260 fluctuation from 2008 to 2016. This trend of SO₂ columns is greatly influenced by the variations of SO₂
261 emissions, since SO₂ emissions also showed an increasing trend from 2005 to 2006, and then
262 decreasing until 2016. The consistency of the trends of SO₂ emissions and concentrations was



263 interrupted in 2011 when the SO₂ concentration reached the highest while the SO₂ emission did not.
264 This inconsistency is mainly because the atmospheric conditions also influence SO₂ concentrations in
265 the atmosphere through changing the chemical reactions with other components and the vertical and
266 horizontal transportations (Uno et al., 2007; Emmons et al., 2010; Schaub et al., 2007). Among the
267 climatic factors, precipitation amount might be a dominant one since it can scavenge the relevant
268 S-related components in the atmosphere. This study also confirmed that the precipitation amount has an
269 obvious negative correlation coefficient (-0.69, $P < 0.05$) with SO₂ concentrations (Fig. 5a). In 2011,
270 the average precipitation amount was only 556.8 mm in China, which was the lowest in the recent 50
271 years (China Climate Bulletin 2011). The lowest dilution effect on ions of precipitation in 2011 might
272 contributed a strong influence on the highest concentrations of SO₂ in the atmosphere. If the year of
273 2011 was excluded, the correlation coefficient between SO₂ emissions and concentrations in the
274 atmosphere would have increased to 0.95 from 0.73 ($P < 0.05$) (Fig. 5b).

275 The ABL NO₂ columns showed a steadily increasing from 2005 to 2011 and then decreasing until to
276 2016 (Fig. 3c). Also, NO_x emissions showed declining from 2011 (China Climate Bulletin 2011, 2012,
277 2013, 2014, 2015, and 2016), which was highly consistent with the trend of NO₂ concentrations (Fig.
278 5d). However, although precipitation had the similar effect on NO₂ in the atmosphere with that on SO₂,
279 precipitation amount did not show a statistically significant negative effect on NO₂ concentrations (Fig.
280 5c). This might mean that the variations of NO₂ concentrations were mainly determined by the
281 emissions in China. The maximum of ABL NO₂ columns also occurred in 2011, which might be caused
282 by both the highest NO_x emissions and the lowest precipitation amounts.

283 The possible reasons for the trends of SO₂ and NO₂ concentrations and emissions have been widely
284 described previously (Ronald et al., 2017; Krotkov et al., 2016), including the economic development



285 and the implements of a series of policies on atmospheric environmental protection. The trends on SO₂
286 and NO₂ directly influenced the variations of acid species in precipitation. The OMI-derived S / N
287 showed a significant decline (17.21 and 10.70 in 2005 and 2016, respectively), indicating the
288 contribution of the sulfate on the precipitation pH has decreased while nitrate contribution is increasing.
289 From 2005 to 2010, the decreasing trend of S / N was due to the slightly decreased SO₂ and rapidly
290 increased NO₂. In 2010, SO₂ decreased by only 1.0% compared with that in 2005, but decreased by
291 10.5% compared with the highest SO₂ concentration in 2007. During the same period, NO₂ increased
292 by 36.9% in 2010. From 2011 to 2016, both of SO₂ and NO₂ declined, but SO₂ had a higher decreasing
293 rate than NO₂ (43.77 molec. cm⁻² yr⁻¹ for SO₂ and 11.39 molec. cm⁻² yr⁻¹ for NO₂). The different
294 decreasing rates induced the further decline of S / N. In 2016, S / N decreased about 37.9% compared
295 with that in 2005.

296 The decreasing trend of SO₄²⁻ / NO₃⁻ in precipitation was also observed from the ground measurements
297 of the national monitoring on acid rains (China Climate Bulletin 2011, 2012, 2013, 2014, 2015, and
298 2016), which showed that the ratio has decreased from 3.80 in 2011 to 2.59 in 2016 (3.49, 3.50, 3.18,
299 2.90 in 2012, 2013, 2014, and 2015, respectively). In some areas of China, such as Jinyunshan, Beijing,
300 Guangzhou, ground measurements also showed that the SO₄²⁻ / NO₃⁻ in precipitation decreased in
301 recent years (Pu et al., 2017; Liu et al., 2016b; Fang et al., 2013).

302 Considering the classification standard of acid types on precipitation (Cheng and Huang, 1998), the
303 precipitation acidity is still dominated by the sulfuric species. The percentages of the areas with
304 sulfuric-nitrous mixed precipitations showed an increasing trend from 9.0% in 2005 to 17.3% in 2016,
305 while the percentages of the areas with sulfuric rains accordingly has decreased. Particularly, the
306 percentage of the areas with S / N > 10 showed a much obvious decreasing trend. The average



307 decreasing rate for the areas with S / N greater than 10 was 1.76 % per year, while the increasing rate
308 for the areas with S / N less 3 was 0.92% yr⁻¹ (Fig. 6). This meant that not only the areas with the
309 sulfuric-nitrous mixed precipitations sprawled, but also the areas with high S / N values shrank with a
310 higher decreasing rate. The whole situation confirmed that the contribution of sulfuric species is getting
311 lower for precipitation acidity in China.

312 Figure 7 shows the trend of S / N for those grid cells that have a statistically significant trend. A large
313 negative trend is visible in China, while only several pixels had a positive trend in Taiwan. This is
314 mainly due to that the environmental regulations on reducing SO₂ emissions were implemented earlier
315 than those on NO_x in China (Ronald et al., 2017). The steadily decreasing trend for SO₂ and the first
316 increasing then decreasing trend for NO₂ resulted in the decrease of S / N in most areas, particularly in
317 east China. The decreasing rate of S / N was within 0-0.25 per year. We should notice that in western
318 China and the north part of Inner Mongolia, the decreasing rates of S / N were relatively higher than
319 those in eastern China. This might not be due to the policies on controlling SO₂ and NO_x emissions, but
320 the rapid increased NO₂ emissions caused by significant socio-economic changes following the
321 National Western Development Strategies (The “Go West” movement) (Cui et al., 2016). NO_x might be
322 getting higher than SO₂ due to their different sources, which decreased the S / N rapidly.

323 3.4. Long-term trends of the potential acidity in precipitation

324 It has confirmed that the SO₂ emissions and concentrations in the atmosphere have decreased since
325 2007. However, the situation of acid rains has not been obviously alleviated since then. According to
326 the statistic, the ratio of cities with occurring acid rains kept relatively stable around 50% from 2005 to
327 2014, but rapidly decreased to about 20% in 2015 and 2016 (Fig. S1). The potential acidity (PA) curve
328 increased first and then decreased (Fig. 8), close to the trend of the ratio of cities with acid rains (R =



329 0.86, $P < 0.05$). Even with the year of 2011 not included, this trend did not change but with different
330 simulated peak years (2008 for 2011 included or 2009 for 2011 excluded). Compared with the highest
331 PA in 2011, 25.5% of acidic ions have been reduced in 2016. If compared with that in 2005, about 11.7%
332 of acidic ions have been reduced in 2016, indicating that some successes on the recovery of acid rain
333 had been achieved.

334 The spatial distribution of potential acidity in 2005, 2010, and 2016 are described in Fig. 9. From the
335 map in 2005, the hotspots occurred in north China extending from the northeast China to the Yangtze
336 delta areas, the highly populated Sichuan Basin, the megacity clusters around Shanghai and Guangzhou.
337 While in 2010, these regions with high potential acidity still existed. Particularly the areas with
338 relatively high potential acidity ranged from 10,001 to 15,000 have obviously expanded around Urumqi
339 in Northwest China. The regions in Xizang and the west Sichuan and Yunnan Province with the
340 potential acidity lower than 5,000 showed an obvious decrease, indicating the PA had increased.

341 Combing the decreased ratio of S / N in western China, the acidic ability should be contributed more by
342 the NO_3^- . This is confirmed in the study of NO_x trends in western China (Cui et al., 2016). The contrary
343 phenomenon was found in Pear River Delta. The potential acidity obviously decreased around the areas
344 of Guangzhou, which was confirmed by the regional monitoring network data in PRD due to the
345 deceased SO_2 emissions (Wang et al., 2013; Fang et al., 2013).

346 Although spatial heterogeneities existed between potential values induced by H_2SO_4 and HNO_3 in 2005
347 and 2010, the PA in 2010 increased by 2.4% compared with that in 2005. Combing the change of S / N
348 from 2005 to 2010, the very close PA values in the two years confirmed that the policy only controlling
349 SO_2 emissions had not an obvious effect on alleviating acid rain pollution. A similar conclusion was
350 obtained through MODELS-3/Community Multiscale Air Quality system (V4.4), in which they



351 concluded that the benefits of SO₂ reductions during 2005-2010 might be negated by increased N
352 emissions (Zhao et al., 2009).

353 On the map of potential acidity in 2016, the spatial pattern has changed greatly from those in 2005 and
354 2010. The hotspots with PA higher than 40,000 are very few, and were mainly located in the northern
355 China. The big hotspot areas in 2010 occurred in Sichuan, Guizhou, and Guangdong Provinces were
356 gone in 2016, and some small hotspot areas in Ningxia, Hubei, Guangxi, Guangdong were also lost,
357 meaning that the PA has significantly decreased in these areas. The heavily acid regions extending from
358 the northeast to the Yangtze areas in 2010 have obviously decreased in 2016. While in the western
359 China, the PA increased around the Urumqi and in Yunnan, Sichuan and Xizang. If the PA increased
360 further in the coming years, the acid pollution might be higher in these regions although PA is still low
361 at present. The increased PA in Western China should be paid attention by the government or the policy
362 makers.

363 It should be noted here that the spatial pattern of PA is not consistent with that of the precipitation pH
364 (Fig S2). The reason for the acidity of precipitation are complex, and many of the primary influencing
365 factors such as sulfide emissions caused by fossil fuel consumption, atmospheric diffusion capacity,
366 and the neutralization capability of atmospheric aerosol have strong regional variations in China (Li,
367 1998). Although the spatial pattern of PA and precipitation pH were different, both of them showed the
368 acid pollution had decreased in 2016 even compared with 2005 and 2010.

369 3.5 Uncertainties

370 Since the ABL SO₂ and NO₂ could indicate the variations of SO₄²⁻ and NO₃⁻ in precipitation, the
371 uncertainty induced by OMI NO₂ columns should be considered in this study. The uncertainty in
372 satellite-based vertical columns is dominated by air mass factors, which have been discussed in detail



373 in a number of previous studies (Boersma et al., 2004; Nowlan et al., 2014; Zyrichidou et al., 2013).

374 Especially in the western China where the values of SO₂ and NO₂ were relative low, errors of the ABL

375 SO₂ and NO₂ columns might be high.

376 This study only considered the potential acidity induced by the SO₄²⁻ and NO₃⁻ the organic acid was not

377 involved. Although the contribution of organic acids to precipitation pH was minor, it could not be

378 neglected, particularly in forest and suburban areas (Stavrakou et al., 2012; Willey et al., 2011). In these

379 areas, the contribution of organic acids on precipitation pH was much higher than in urban areas.

380 This study mainly discussed the change of acidic species in precipitations, but the neutralization should

381 be fully considered when the precipitation pH is studied. The implementation of particulate matter

382 reduction policy has not only resulted in the decreasing trend of the acid-related compound, but also the

383 decrease of alkaline species in precipitation (Zhao et al., 2009; Wang et al., 2012; Tang et al., 2010).

384 However, the neutralizing is not considered in this study.

385 4. Conclusions

386 The effect of national NO_x and SO₂ policies on acid components in precipitation was assessed in China,

387 based on the OMI ABL SO₂ and NO₂ columns. The OMI information on S and N obtained a reliable

388 indicator on the variations of SO₄²⁻ / NO₃⁻ in precipitation. The long-term trend of S / N in precipitation

389 significantly decreased from 2005 to 2016 in China, which meant the contribution of nitrates getting

390 higher on precipitation pH. This decline of S / N in precipitation was mainly due to the national NO_x

391 and SO₂ policies enacted at different times. Under such policies, SO₂ showed a decreasing trend while

392 NO₂ showed the increasing first then decreasing trend from 2005 to 2016. The ABL SO₂ and NO₂

393 columns had a good consistency with those of emissions, but they were also greatly influenced by the

394 precipitation amounts. Particularly for the year of 2011, SO₂ and NO₂ got their peaks, respectively,



395 mainly due to the joint contribution from the lowest precipitation amounts and high emissions in 2011.

396 The spatial distribution of S / N in precipitation showed considerable regional variations in China. The

397 low values were mainly located in East China, and the areas around Urumqi in Northwest China, which

398 is close to the spatial distribution of population densities. The highly developed traffics in the densely

399 populated areas, and the more widespread application of the FGD than SCR in power units might be

400 the main reasons for the low S / N in the mentioned regions.

401 The potential acidity of S and N in precipitation increased first from 2005 to 2011 and then decreased

402 from 2011 to 2016. The increased PA indicated that the benefits of SO₂ reductions during 2005-2010

403 might be offset by increased N emissions obtained by the previous studies, while the decreased PA

404 from 2011 to 2016 indicated that the national NO_x and SO₂ policies issued in 12th Five Plan are in

405 effect.

406 **Author contribution**

407 Xiuying Zhang conceived and designed the methodology and wrote the paper with Dongmei Chen. Lei

408 Liu, Limin Zhao, and Wuting Zhang help to process the data sets.

409 **Acknowledgements**

410 This study is supported by the National Natural Science Foundation of China (No. 41471343), and the

411 Fundamental Research Funds for the Central Universities (0904-14380013). We acknowledge the free

412 use of tropospheric NO₂ column and ABL SO₂ column from the OMI sensor from www.temis.nl. We

413 also thank Louisa Emmons from National Center for Atmospheric Research (NCAR) for providing the

414 MOZART output data.

415 **Competing interests**

416 The authors declare that they have no conflict of interest.

417 **Reference**

- 418 Boersma, K. F., Eskes, H. J., and Brinkma, E. J.: Error analysis for tropospheric NO₂ retrieval from
419 space, *Journal of Geophysical Research-Atmospheres*, 109, doi:10.1029/2003JD003962., 2004.
- 420 Boersma, K. F., Eskes, H. J., Dirksen, R. J., van der A, R. J., Veefkind, J. P., Stammes, P., Huijnen, V.,
421 Kleipool, Q. L., Sneep, M., Claas, J., Leitao, J., Richter, A., Zhou, Y., and Brunner, D.: An improved
422 tropospheric NO₂ column retrieval algorithm for the Ozone Monitoring Instrument, *Atmospheric*
423 *Measurement Techniques*, 4, 1905-1928, 10.5194/amt-4-1905-2011, 2011.
- 424 Charlson, R. J., and Rodhe, H.: FACTORS CONTROLLING THE ACIDITY OF NATURAL
425 RAINWATER, *Nature*, 295, 683-685, 10.1038/295683a0, 1982.
- 426 Chen, D., Feng, Y., and Zhang, X.: Comparison of variability and change rate in tropospheric NO₂
427 column obtained from satellite products across China during 1997-2015, *International Journal of*
428 *Digital Earth*, 10, 814-828, 10.1080/17538947.2016.1252435, 2017.
- 429 Cheng, X., and Huang, M.: A Classification Method to Analyze the Chemical Characteristics of
430 Precipitation, *Climatic and Environmental Research*, 3, 7, 1998.
- 431 Cui, Y., Lin, J., Song, C., Liu, M., Yan, Y., Xu, Y., and Huang, B.: Rapid growth in nitrogen dioxide
432 pollution over Western China, 2005-2013, *Atmospheric Chemistry and Physics*, 16, 6207-6221,
433 10.5194/acp-16-6207-2016, 2016.
- 434 de Foy, B., Lu, Z., and Streets, D. G.: Satellite NO₂ retrievals suggest China has exceeded its NO_x
435 reduction goals from the twelfth Five-Year Plan, *Scientific Reports*, 6, 10.1038/srep35912, 2016.
- 436 Duan, L., Yu, Q., Zhang, Q., Wang, Z., Pan, Y., Larssen, T., Tang, J., and Mulder, J.: Acid deposition in
437 Asia: Emissions, deposition, and ecosystem effects, *Atmospheric Environment*, 146, 55-69,
438 10.1016/j.atmosenv.2016.07.018, 2016.
- 439 Emmons, L. K., Walters, S., Hess, P. G., Lamarque, J. F., Pfister, G. G., Fillmore, D., Granier, C.,
440 Guenther, A., Kinnison, D., Laepple, T., Orlando, J., Tie, X., Tyndall, G., Wiedinmyer, C., Baughcum,
441 S. L., and Kloster, S.: Description and evaluation of the Model for Ozone and Related chemical Tracers,
442 version 4 (MOZART-4), *Geoscientific Model Development*, 3, 43-67, 2010.
- 443 Fang, Y., Wang, X., Zhu, F., Wu, Z., Li, J., Zhong, L., Chen, D., and Yoh, M.: Three-decade changes in
444 chemical composition of precipitation in Guangzhou city, southern China: has precipitation recovered
445 from acidification following sulphur dioxide emission control?, *Tellus Series B-Chemical and Physical*



- 446 Meteorology, 65, 10.3402/tellusb.v65i0.20213, 2013.
- 447 He, X.-h., Xu, X.-b., Yu, X.-l., and Tang, J.: Concentrations and Acidity Contributions of Acetate and
448 Formate in Precipitation at 14 Stations of China, Huanjing Kexue, 31, 858-864, 2010.
- 449 Huang, D.-Y., Xu, Y.-G., Peng, P. a., Zhang, H.-H., and Lan, J.-B.: Chemical composition and seasonal
450 variation of acid deposition in Guangzhou, South China: Comparison with precipitation in other major
451 Chinese cities, Environmental Pollution, 157, 35-41, 10.1016/j.envpol.2008.08.001, 2009.
- 452 Huang, Y., Wang, Y., and Zhang, L.: Long-term trend of chemical composition of wet atmospheric
453 precipitation during 1986-2006 at Shenzhen City, China, Atmospheric Environment, 42, 3740-3750,
454 10.1016/j.atmosenv.2007.12.063, 2008.
- 455 Khwaja, H. A., and Husain, L.: Chemical characterization of acid precipitation in Albany, New-York,
456 Atmospheric Environment Part a-General Topics, 24, 1869-1882, 10.1016/0960-1686(90)90519-s,
457 1990.
- 458 Krotkov, N. A., McLinden, C. A., Li, C., Lamsal, L. N., Celarier, E. A., Marchenko, S. V., Swartz, W.
459 H., Bucsela, E. J., Joiner, J., Duncan, B. N., Boersma, K. F., Veefkind, J. P., Levelt, P. F., Fioletov, V. E.,
460 Dickerson, R. R., He, H., Lu, Z., and Streets, D. G.: Aura OMI observations of regional SO₂ and NO₂
461 pollution changes from 2005 to 2015, Atmospheric Chemistry and Physics, 16, 4605-4629,
462 10.5194/acp-16-4605-2016, 2016.
- 463 Kuribayashi, M., Ohara, T., Morino, Y., Uno, I., Kurokawa, J.-i., and Hara, H.: Long-term trends of
464 sulfur deposition in East Asia during 1981-2005, Atmospheric Environment, 59, 461-475,
465 10.1016/j.atmosenv.2012.04.060, 2012.
- 466 Lamsal, L. N., Duncan, B. N., Yoshida, Y., Krotkov, N. A., Pickering, K. E., Streets, D. G., and Lu, Z.:
467 U.S. NO₂ trends (2005-2013): EPA Air Quality System (AQS) data versus improved observations from
468 the Ozone Monitoring Instrument (OMI), Atmospheric Environment, 110, 130-143,
469 10.1016/j.atmosenv.2015.03.055, 2015.
- 470 Larssen, T., and Carmichael, G. R.: Acid rain and acidification in China: the importance of base cation
471 deposition, Environmental Pollution, 110, 89-102, 10.1016/s0269-7491(99)00279-1, 2000.
- 472 Lee, C., Martin, R. V., van Donkelaar, A., Lee, H., Dickerson, R. R., Hains, J. C., Krotkov, N., Richter,
473 A., Vinnikov, K., and Schwab, J. J.: SO₂ emissions and lifetimes: Estimates from inverse modeling
474 using in situ and global, space-based (SCIAMACHY and OMI) observations, Journal of Geophysical
475 Research: Atmospheres, 116, 1-13, 10.1029/2010JD014758, 2011.



- 476 Levelt, P. F., Van den Oord, G. H. J., Dobber, M. R., Malkki, A., Visser, H., de Vries, J., Stammes, P.,
477 Lundell, J. O. V., and Saari, H.: The Ozone Monitoring Instrument, *Ieee Transactions on Geoscience*
478 *and Remote Sensing*, 44, 1093-1101, 10.1109/tgrs.2006.872333, 2006.
- 479 Li, J.: Spatial distribution of acid deposition flux of precipitation in China, *Research of Environmental*
480 *Sciences*, 11, 4, 1998.
- 481 Li, Y. H., Wang, D., Xu, X. T., Gao, X. X., Sun, X., and Xu, N. J.: Physiological responses of a green
482 algae (*Ulva prolifera*) exposed to simulated acid rain and decreased salinity, *Photosynthetica*, 55,
483 623-629, 10.1007/s11099-017-0689-0, 2017.
- 484 Liu, F., Zhang, Q., Ronald, J. v. d. A., Zheng, B., Tong, D., Yan, L., Zheng, Y., and He, K.: Recent
485 reduction in NO_x emissions over China: synthesis of satellite observations and emission inventories,
486 *Environmental Research Letters*, 11, 10.1088/1748-9326/11/11/114002, 2016a.
- 487 Liu, L., Zhang, X., and Lu, X.: The composition, seasonal variation, and potential sources of the
488 atmospheric wet sulfur (S) and nitrogen (N) deposition in the southwest of China, *Environmental*
489 *Science and Pollution Research*, 23, 6363-6375, 10.1007/s11356-015-5844-1, 2016b.
- 490 Liu, L., Zhang, X., Wang, S., Lu, X., and Ouyang, X.: A Review of Spatial Variation of Inorganic
491 Nitrogen (N) Wet Deposition in China, *Plos One*, 11, 10.1371/journal.pone.0146051, 2016c.
- 492 Liu, L., Zhang, X., Wang, S., Zhang, W., and Lu, X.: Bulk sulfur (S) deposition in China, *Atmospheric*
493 *Environment*, 135, 41-49, 10.1016/j.atmosenv.2016.04.003, 2016d.
- 494 Liu, L., Zhang, X., Xu, W., Liu, X., Lu, X., Chen, D., Zhang, X., Wang, S., and Zhang, W.: Estimation
495 of monthly bulk nitrate deposition in China based on satellite NO₂ measurement by the Ozone
496 Monitoring Instrument, *Remote Sensing of Environment*, 199, 14, 2017.
- 497 Nowlan, C. R., Martin, R. V., Philip, S., Lamsal, L. N., Krotkov, N. A., Marais, E. A., Wang, S., and
498 Zhang, Q.: Global dry deposition of nitrogen dioxide and sulfur dioxide inferred from space-based
499 measurements, *Global Biogeochemical Cycles*, 28, 1025-1043, 10.1002/2014gb004805, 2014.
- 500 Pu, W., Quan, W., Ma, Z., Shi, X., Zhao, X., Zhang, L., Wang, Z., and Wang, W.: Long-term trend of
501 chemical composition of atmospheric precipitation at a regional background station in Northern China,
502 *Science of the Total Environment*, 580, 1340-1350, 10.1016/j.scitotenv.2016.12.097, 2017.
- 503 Racette, P., Adler, R. F., Gasiewski, A. J., Jakson, D. M., and Zacharias, D. S.: An airborne
504 millimeter-wave imaging radiometer for cloud, precipitation, and atmospheric water vapor studies,
505 *Journal of Atmospheric and Oceanic Technology*, 13, 610-619,



- 506 10.1175/1520-0426(1996)013<0610:aamwir>2.0.co;2, 1996.
- 507 Rodhe, H., Dentener, F., and Schulz, M.: The global distribution of acidifying wet deposition,
508 Environmental Science & Technology, 36, 4382-4388, 10.1021/es020057g, 2002.
- 509 Ronald, J. v. d. A., Mijling, B., Ding, J., Koukouli, M. E., Liu, F., Li, Q., Mao, H., and Theys, N.:
510 Cleaning up the air: effectiveness of air quality policy for SO₂ and NO_x emissions in China,
511 Atmospheric Chemistry and Physics, 17, 1775-1789, 10.5194/acp-17-1775-2017, 2017.
- 512 Schaub, D., Brunner, D., Boersma, K. F., Keller, J., Folini, D., Buchmann, B., Berresheim, H., and
513 Staehelin, J.: SCIAMACHY tropospheric NO₂ over Switzerland: estimates of NO_x lifetimes and
514 impact of the complex Alpine topography on the retrieval, Atmospheric Chemistry and Physics, 7,
515 5971-5987, 2007.
- 516 Shi, C., Qiu, M., Zhang, A., Zhang, H., Zhang, S., and Wang, Z.: Spatiotemporal Trends and the Impact
517 Factors of Acid Rain in Anhui Province, Environmental Science, 31, 7, 2010.
- 518 Song, H., and Yang, M.: Analysis on Effectiveness of SO₂ Emission Reduction in Shanxi, China by
519 Satellite Remote Sensing, Atmosphere, 5, 830-846, 10.3390/atmos5040830, 2014.
- 520 Stavrakou, T., Mueller, J. F., Peeters, J., Razavi, A., Clarisse, L., Clerbaux, C., Coheur, P. F., Hurtmans,
521 D., De Maziere, M., Vigouroux, C., Deutscher, N. M., Griffith, D. W. T., Jones, N., and Paton-Walsh,
522 C.: Satellite evidence for a large source of formic acid from boreal and tropical forests, Nature
523 Geoscience, 5, 26-30, 10.1038/ngeo1354, 2012.
- 524 Tang, J., Xu, X., Ba, J., and Wang, S.: Trends of the precipitation acidity over China during 1992-2006,
525 Chinese Science Bulletin, 55, 1800-1807, 10.1007/s11434-009-3618-1, 2010.
- 526 Theys, N., De Smedt, I., van Gent, J., Danckaert, T., Wang, T., Hendrick, F., Stavrakou, T., Bauduin, S.,
527 Clarisse, L., Li, C., Krotkov, N., Yu, H., Brenot, H., and Van Roozendael, M.: Sulfur dioxide vertical
528 column DOAS retrievals from the Ozone Monitoring Instrument: Global observations and comparison
529 to ground-based and satellite data, Journal of Geophysical Research-Atmospheres, 120, 2470-2491,
530 10.1002/2014jd022657, 2015.
- 531 Uno, I., He, Y., Ohara, T., Yamaji, K., Kurokawa, J. I., Katayama, M., Wang, Z., Noguchi, K.,
532 Hayashida, S., Richter, A., and Burrows, J. P.: Systematic analysis of interannual and seasonal
533 variations of model-simulated tropospheric NO₂ in Asia and comparison with GOME-satellite data,
534 Atmospheric Chemistry and Physics, 7, 1671-1681, 2007.
- 535 Vet, R., Artz, R. S., Carou, S., Shaw, M., Ro, C.-U., Aas, W., Baker, A., Bowersox, V. C., Dentener, F.,



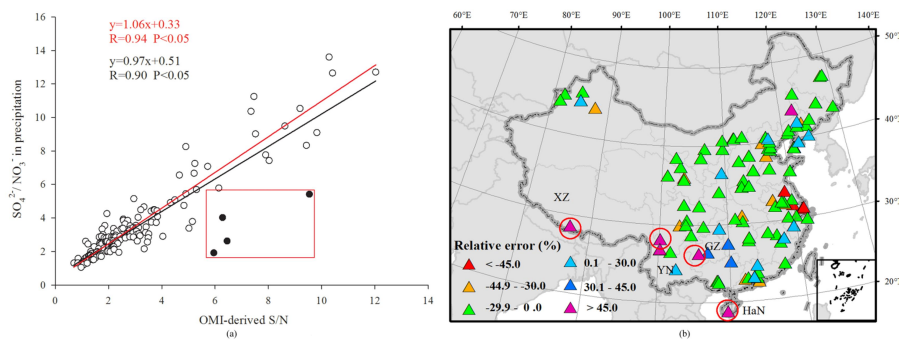
- 536 Galy-Lacaux, C., Hou, A., Pienaar, J. J., Gillett, R., Cristina Forti, M., Gromov, S., Hara, H., Khodzher,
537 T., Mahowald, N. M., Nickovic, S., Rao, P. S. P., and Reid, N. W.: A global assessment of precipitation
538 chemistry and deposition of sulfur, nitrogen, sea salt, base cations, organic acids, acidity and pH, and
539 phosphorus, *Atmospheric Environment*, 93, 3-100, 10.1016/j.atmosenv.2013.10.060, 2014.
- 540 Wang, S. X., Zhao, B., Cai, S. Y., Klimont, Z., Nielsen, C. P., Morikawa, T., Woo, J. H., Kim, Y., Fu, X.,
541 Xu, J. Y., Hao, J. M., and He, K. B.: Emission trends and mitigation options for air pollutants in East
542 Asia, *Atmospheric Chemistry and Physics*, 14, 6571-6603, 10.5194/acp-14-6571-2014, 2014.
- 543 Wang, W., and Xu, J.: Research Progress in Precipitation Chemistry in China, *Progress in Chemistry*,
544 21, 266, 2009.
- 545 Wang, X., Liu, H., Pang, J., Carmichael, G., He, K., Fan, Q., Zhong, L., Wu, Z., and Zhang, J.:
546 Reductions in sulfur pollution in the Pearl River Delta region, China: Assessing the effectiveness of
547 emission controls, *Atmospheric Environment*, 76, 113-124, 10.1016/j.atmosenv.2013.04.074, 2013.
- 548 Wang, Y., Yu, W., Pan, Y., and Wu, D.: Acid neutralization of precipitation in Northern China, *Journal*
549 *of the Air & Waste Management Association*, 62, 204-211, 10.1080/10473289.2011.640761, 2012.
- 550 Willey, J. D., Glinski, D. A., Southwell, M., Long, M. S., Avery, G. B., Jr., and Kieber, R. J.: Decadal
551 variations of rainwater formic and acetic acid concentrations in Wilmington, NC, USA, *Atmospheric*
552 *Environment*, 45, 1010-1014, 10.1016/j.atmosenv.2010.10.047, 2011.
- 553 Wu, Y., Zhang, S., Hao, J., Liu, H., Wu, X., Hu, J., Walsh, M. P., Wallington, T. J., Zhang, K. M., and
554 Stevanovic, S.: On-road vehicle emissions and their control in China: A review and outlook, *Science of*
555 *the Total Environment*, 574, 332-349, 10.1016/j.scitotenv.2016.09.040, 2017.
- 556 Xie, Z., Du, Y., Zeng, Y., Li, Y., Yan, M., and Jiao, S.: Effects of precipitation variation on severe acid
557 rain in southern China, *Journal of Geographical Sciences*, 12, 2009.
- 558 Yu, H., He, N., Wang, Q., Zhu, J., Xu, L., Zhu, Z., and Yu, G.: Wet acid deposition in Chinese natural
559 and agricultural ecosystems: Evidence from national-scale monitoring, *Journal of Geophysical*
560 *Research-Atmospheres*, 121, 10995-11005, 10.1002/2015jd024441, 2016.
- 561 Zhang, X., Jiang, H., Jin, J., Xu, X., and Zhang, Q.: Analysis of acid rain patterns in northeastern China
562 using a decision tree method, *Atmospheric Environment*, 46, 590-596, 10.1016/j.atmosenv.2011.03.004,
563 2012.
- 564 Zhao, B., Wang, S., Wang, J., Fu, J. S., Liu, T., Xu, J., Fu, X., and Hao, J.: Impact of national NO_x and
565 SO₂ control policies on particulate matter pollution in China, *Atmospheric Environment*, 77, 453-463,



- 566 10.1016/j.atmosenv.2013.05.012, 2013.
- 567 Zhao, Y., Duan, L., Xing, J., Larssen, T., Nielsen, C. P., and Hao, J.: Soil Acidification in China: Is
- 568 Controlling SO₂ Emissions Enough?, *Environmental Science & Technology*, 43, 8021-8026,
- 569 10.1021/es901430n, 2009.
- 570 Zyrichidou, I., Koukouli, M. E., Balis, D. S., Kioutsoukis, I., Poupkou, A., Katragkou, E., Melas, D.,
- 571 Boersma, K. F., and van Roozendaal, M.: Evaluation of high resolution simulated and OMI retrieved
- 572 tropospheric NO₂ column densities over Southeastern Europe, *Atmospheric Research*, 122, 55-66,
- 573 10.1016/j.atmosres.2012.10.028, 2013.
- 574



575



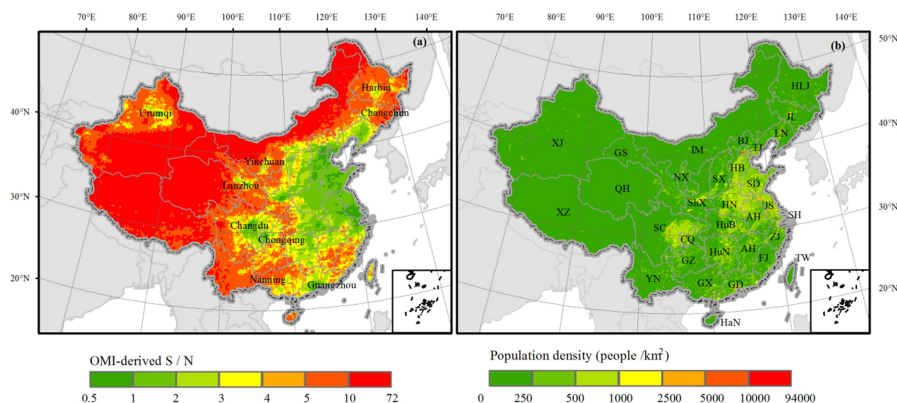
576

577

578

579

Fig. 1. (a) Scatter plots of the OMI-derived S / N and the collected $\text{SO}_4^{2-} / \text{NO}_3^-$ in precipitation; (b) spatial distribution of the relative errors between the OMI-derived S / N and the collected ratio of $\text{SO}_4^{2-} / \text{NO}_3^-$ in precipitation



580

581

582

583

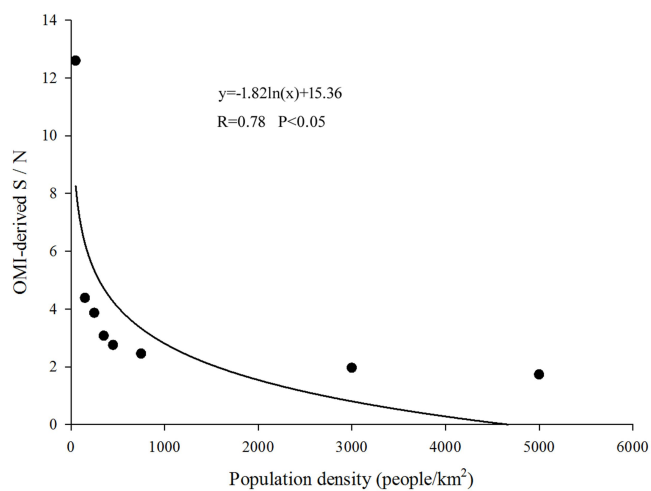
584

585

586

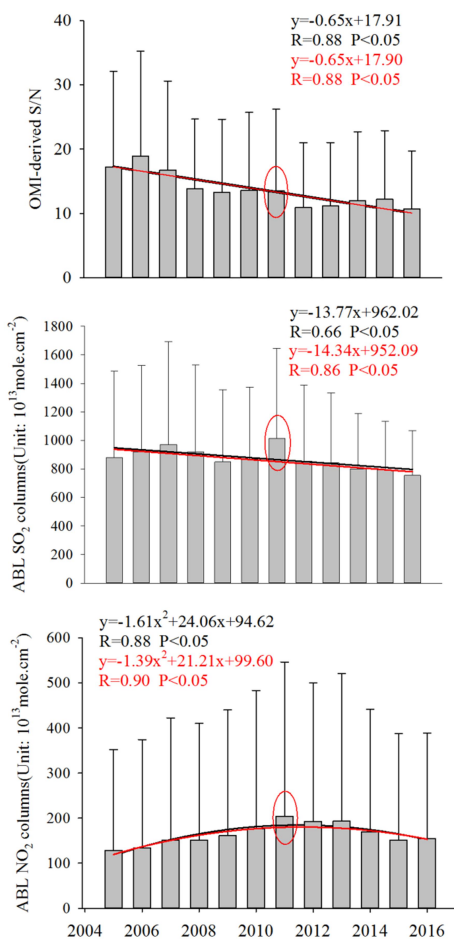
587

Fig. 2. Spatial distribution of (a) OMI-derived S/N in 2016 and (b) the population density in China. The successfully full provincial names are Beijing (BJ), Tianjin (TJ), Hebei (HeB), Shandong (SD), Shanxi (SX), Henan (HeN), Shaanxi (SaX), Liaoning (LN), Jilin (JL), Heilongjiang (HLJ), Neimenggu (NMG), Gansu (GS), Ningxia (NX), Xinjiang (XJ), Shanghai (SH), Jiangsu (JS), Zhejiang (ZJ), Anhui (AH), Hubei (HuB), Hunan (HuN), Jiangxi (JX), Fujian (FJ), Guangdong (GD), Hainan (HaN), Yunnan (YN), Guizhou (GZ), Chongqing (CQ), Sichuan (SC), Guangxi (GX), Xizang (XZ), Qinghai (QH), and Taiwan (TW).



588
589

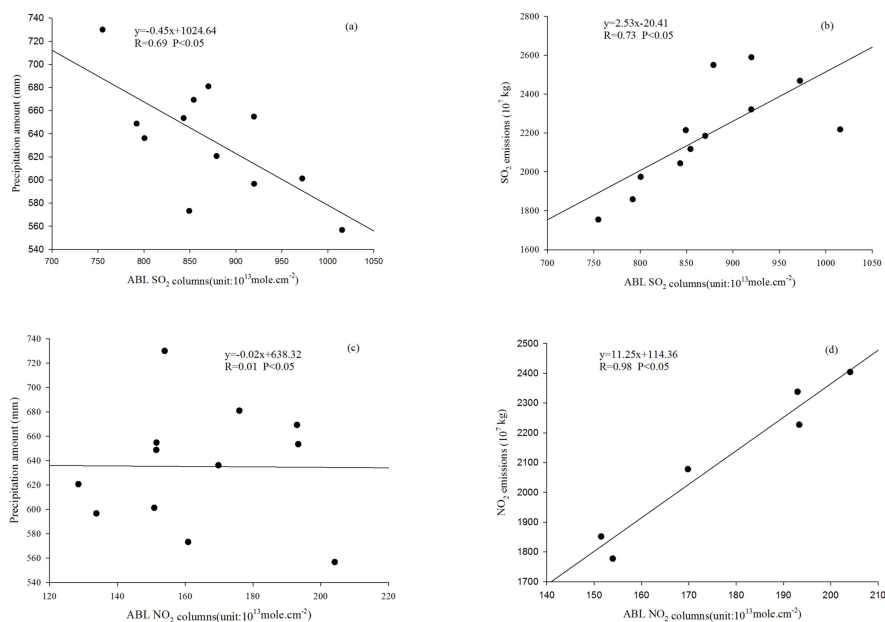
Fig. 3. Relationship between Omi-derived S / N and population density



590

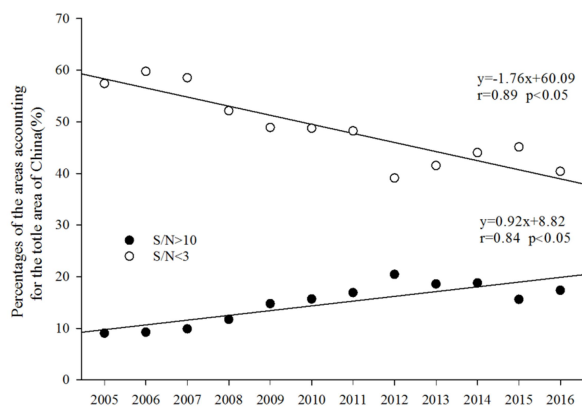
591

Fig. 4. Long-term trends of OMI-derived S / N, ABL SO₂ columns, ABL NO₂ columns from 2005 to 2016 in China



592
593
594
595

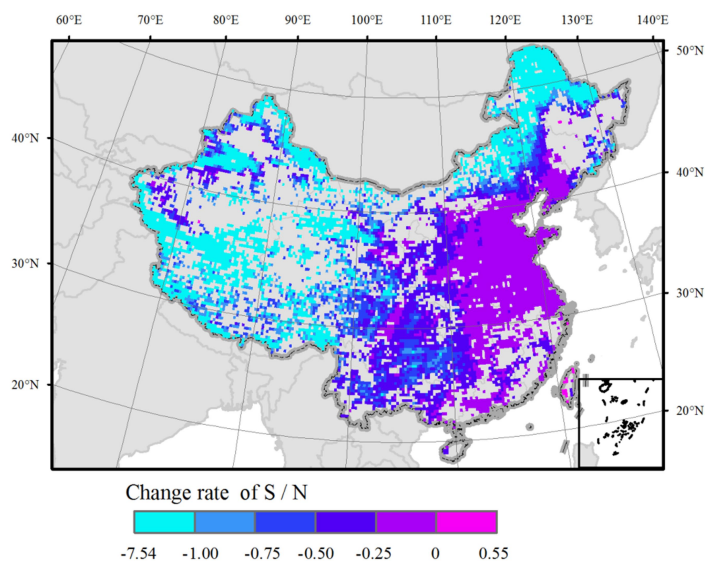
Fig. 5. Relationship between the (a) ABL SO₂ columns and precipitation amounts, (b) ABL SO₂ columns and SO₂ emissions, (c) ABL NO₂ columns and precipitation amounts, (d) ABL NO₂ columns and NO_x emissions



596

597

Fig.6. Percentages of the areas with mixed acidic precipitation types from 2005 to 2016

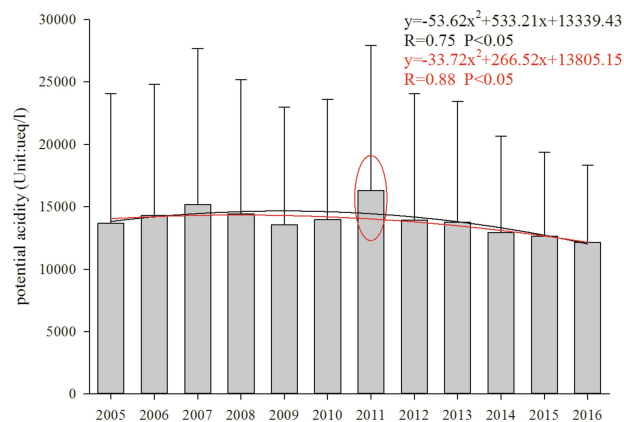


598

599

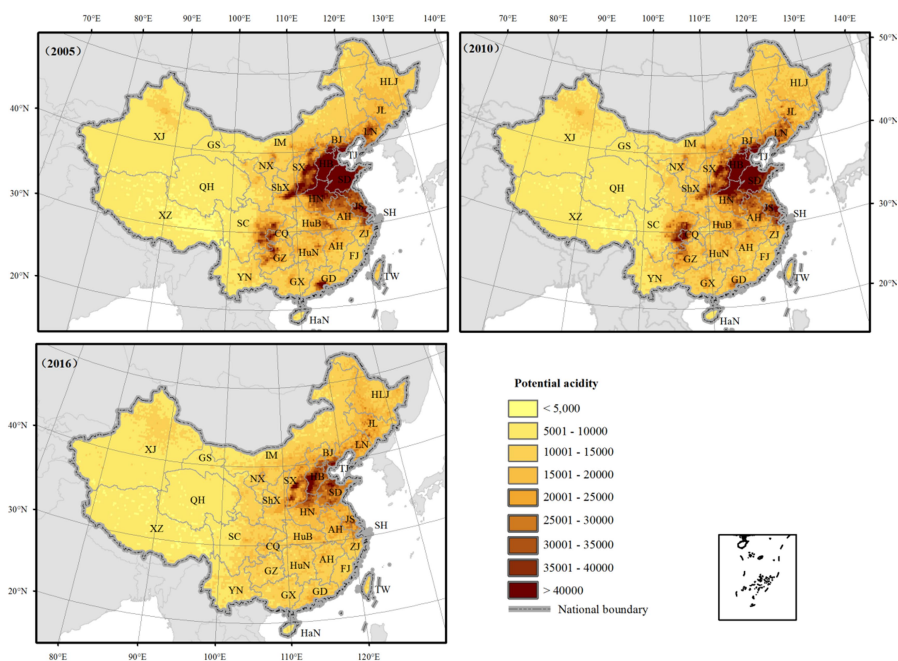
600

Fig.7. Linear trend per year for the ratio of OMI-derived S/N in from 2005 to 2016 derived from OMI. For the light grey areas no significant trend has been found in the time series.



601
602
603
604

Fig. 8. Trends of potential acidity induced by SO_4^{2-} and NO_3^- from 2005 to 2016 in China



605

606

607

608

609

Fig. 9. Spatial distributions of potential acidity in 2005, 2010, and 2016 in China. The successfully full provincial names are the same with Fig. 2.